Proceedings of 8 ICSHMO, Foz do Iguaçu, Brazil, April 24-28, 2006, INPE, p. 753-757.

NORTHWARD-PROPAGATING SURGES EAST OF THE ANDES DURING THE SALLJEX

José M. Gálvez[1] and Michael W. Douglas[2]

[1] *CIMMS/University of Oklahoma, Norman, OK 73069*
[2] *NSSL/NOAA, Norman, OK 73069*

1. INTRODUCTION

The entire western edge of South America is shaped by the Andes (Figure 1), a narrow but steep mountain range that extends from northern Venezuela (10°N) to southern Chile (54°S). The width of the Andes ranges from 100 to 600 km and the elevation from 200 to almost 700 mASL. Along the east flank of the Andes, a wide flat and low-altitude corridor extends and will be henceforth referred as the Central South American Corridor (CSAC). The CSAC covers the Venezuelan-Colombian llanos (9°N to 5°N); the western Amazon rainforest along Colombia, Ecuador, Peru, western Brazil and Bolivia (4°N to 15°S); the Chaco of Bolivia, Paraguay and Argentina (16°S to 30°S) and the Argentinean-Uruguayan Pampas (30°S to 42°S). The approximate elevation and width of this corridor vary between 100 and 500 mASL, and 500 to 1000 km respectively. The Andes represent a topographic barrier that not only divides Pacific maritime air masses from those over the Atlantic and Amazonia, but also produces a variety of mesometeorological phenomena such as upslope and downslope events, lee cyclogenesis, gravity waves and trapped downgradient flows. The Andes bends at 18°S from a north-south orientation to the south to a northwest-southeast orientation north of this latitude. Herein, this bend will be referred as the 'Andean elbow'.

* *Corresponding author address: José M. Gálvez CIMMS/OU, 1313 Halley Circle, Norman OK, 73069. Email: Jose.Galvez@noaa.gov*

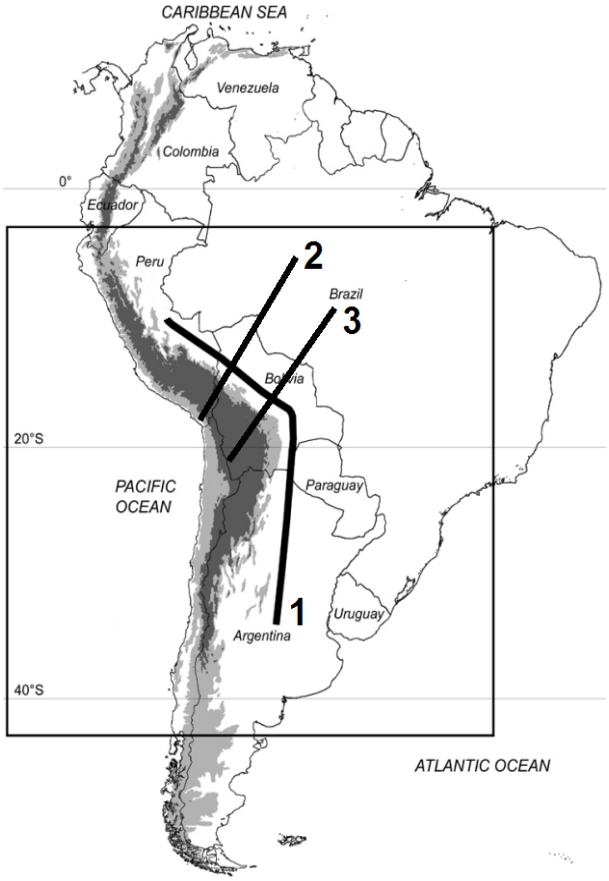

Figure 1. Map of South America including country boundaries and names. The domain of study is indicated with a box. Elevations along the Andes that range between 1000 and 3000 mASL are shaded with light gray and those higher than 3000 mASL with dark gray. Thick black lines indicate the position of an along-surge cross section (1) and two across-surge cross sections (2 and 3) presented later.

Northward-propagating surges occur all year round over the CSAC and have been documented by different authors. They transport mid-latitude cool and dry air masses from central Argentina into Paraguay, Bolivia, Brazil and Peru. The signal of these surges is sometimes visible as far north as Ecuador, Colombia and Venezuela (Parmenter, 1976) in the form of a change in the meridional component of the wind from northerly to southerly, generally accompanied with a decrease in convective activity behind the leading edge of the surge. During the austral winter, the major impacts of these surges are freezing conditions from central Argentina to southern Brazil and Bolivia (Vera and Vigliariolo, 2000; Garreaud, 2000), which are harmful to the Southern Brazil coffee production (Hamilton and Tarifa, 1978; Marengo et al., 1997). During the warm season their interaction with very moist air ahead leads to heavy rainfall events produced by deep convection in the leading edge of the cool air (Garreaud, 2000).

The mechanisms that control the generation and evolution of South American cold surges have also been considered in the literature. Krishnamurti et al. (1999) indicated the presence of a large-amplitude trough in the mid-latitude westerlies during frost events in southeastern Brazil. This trough, associated with synoptic and planetary scale events, generally penetrates well into the tropics. Garreaud (1999, 2000) also indicated that the frost events in Brazil occur during periods when the large-scale environment is characterized by a developing mid-latitude wave in the middle and upper troposphere, with a ridge immediately west of the Andes and a downstream trough over eastern South America. As the system develops, the presence of a transient cold anticyclone over the subtropical plains of the continent emerges as a key element of the equatorward migration of the system. The blocking effect of the Andes leads to an ageostrophic, low-level southerly flow that advects cold air into the subtropics. As the air moves north, the blocking effect of the Andes weakens because the adjustment back to geostrophy decreases towards the equator, and adding the effects of the Andean elbow, the cold air spreads out into the tropics. The author also mentioned that the characteristics of the surges are similar to those observed in the lee of the Rocky Mountains. Colle and Mass (1995), among with others, indicated the presence of different types of phenomena associated with these events. They listed Kelvin or topographically trapped gravity waves, topographic Rossby waves, topographically trapped downgradient flows and density currents.

The present study has as the main goal to describe the characteristics of the southerly surge event that occurred east of the Andes during the period of 22-25 January 2003 using observations collected during the South American Low Level Jet Experiment (SALLJEX 2002-3), and a numerical simulation using the Weather Research and Forecasting (WRF) model. The SALLJEX special observations include pilot balloon and radiosondes as well as flight level data from a NOAA-P3 research aircraft. The focus will be to provide a preliminary answer to the question 'Which types of mesoscale phenomena can be associated with the 22-25 January 2003 southerly surge?' based on theoretical, observational and simulation results.

2. METHODOLOGY

Wind observations from operational radiosonde and an enhanced upper air network established during the SALLJEX, together with the observation from a NOAA P-3 research aircraft are used to decribe the surge. Unfortunately, the spatial and temporal resolution of these datasets is limited to describe the processes that occur on the mesoscale. Only the NOAA P-3 measurements had mesoscale or better spatial resolution and these were made only during one flight per day. To evaluate changes with better resolution than the observations could provide, a 72-hour long simulation was carried out using the WRF model. The horizontal resolution of the WRF was set to 30 km, and the vertical resolution to 31 sigma levels. Table 1 displays the physical and dynamical options selected for the simulation. The initial and boundary conditions were extracted from the NCEP Global Tropospheric Analyses (NGTA). These are 1° global analyses constructed 6 hours after the operational analyses to assimilate a larger number of delayed observations and therefore to represent the atmospheric structure more accurately. The NGTA boundary conditions were available every 6 hours and were therefore interpolated linearly in time to fit the 3-minute time step of the model. The simulation was initialized at 00 UTC on 23 January 2003 (21 LST Argentina on the 22), during the onset of the surge event.

3. RESULTS

The horizontal structure and temporal evolution of the southerly surge are summarized in figures 2 through 4. The analyses displayed were constructed for 925 mb, since the largest gradients were observed at low levels. Figure 2 is a comparison between upper air wind observations from pilot balloons and radiosondes with model simulations. The left panel shows te evolution of the flow from January 23 2003 at 00UTC (top) through January 25 2003 at 00 UTC (bottom). The right panels show the simulated meridional wind field for the corresponding times. Significant agreement can be noticed between the direction and the speed of the observed and the simulated winds.

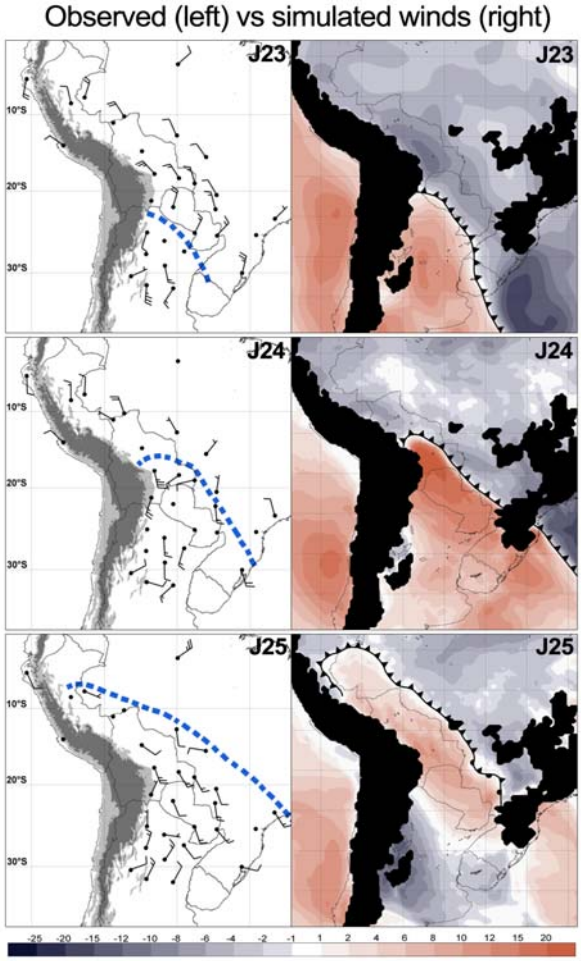

Figure 2. 925 mb observed winds in kt (left) and meridional component of the WRF model simulated wind in m s^{-1} (right) for 23 January 2003 at 00 UTC (top), 24 January 2003 at 00 UTC (center) and 25 January 2003 at 00 UTC (bottom). The location of the windshift is sketched. Terrain above 1000 m is shaded in black.

The surge propagated from northern Argentina (~22°S) into northern Peru (~4°S) in a matter of 48 hours. This gives a mean meridional displacement of +9° day^{-1}. The largest wind speeds were observed and simulated immediately east of the Andes. They peaked at 00 UTC January 24, when the edge of the surge when the edge of the surge was located immediately north from the Andean elbow. Figure 3 shows an analysis constructed using the NOAA P-3 research aircraft. The analysis indicates that the highest wind speeds measured at 15 UTC January 24 were in the order of 25 m s^{-1} and located just north of the Andean elbow in central Bolivia. The thermal structure of this austral summer southerly surge exhibited, as suggested by the literature, very little (i.e. almost unnoticeable) difference with respect to the air ahead of it. The largest difference, other than the wind shift, was observed in the moisture field, evident in figure 3, where the dewpoint decreases from 16°C to 12°C over a distance of 80 km just east of the Andean elbow.

a. Initial down-gradient flow characteristics

Figure 4 summarizes the simulated propagation of the surge in terms of the mixing ratio and geopotential height at 925 mb (closely related to the pressure reduced to sea level). The edge of the wind shift is sketched based on the meridional wind field (see figure 2 for an example). Figure 4 suggests that the southerly surge behaved as a topographically trapped downgradient flow, process described in previous studies over the region, since the pressure gradient was not perpendicular to the mountain barrier and yet the flow was parallel to the Andes (Figure 4, top left panel). This indicates the presence of ageostrophic motions.

Though evident, the blocking effects of the Andes were quantified using the following Froude number expression from Bluestein (1993):

$$F^2 = U^2 / N^2 H^2$$

where U is the upslope component of the wind in m s^{-1}, N is the Brunt-Vaisala frequency in s^{-1} and H is the altitude of the eastern mountain range in m. Using a Brunt-Vaisala frequency of 0.018 s^{-1}, and an average altitude of 4500 mASL as the elevation of the eastern mountain range, it was calculated that for the flow to become supercritical and overcome the Andes ($F \geq 1$), 80 m s^{-1} across-Andes winds would be necessary.

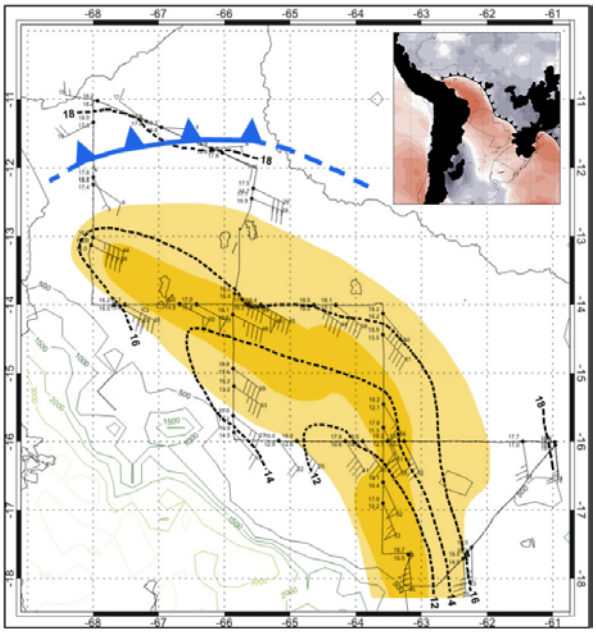

Figure 3. 925mb dewpoint temperature in °C (dashed) and winds in kt (barbs) measured with the NOAA P-3 Research Aircraft around 15Z on January 24 2003, as part of the SALLJEX. The winds stronger than 30 and 50 kt are shaded in yellow and dark yellow respectively. The edge of the wind shift is indicated with a blue cold-front icon. The 925 meridional wind map computed by the model is presented to the right and top of the figure.

b. Establishment of a barrier jet

Towards recovering geostrophic balance, the surge deflects towards the northwest as soon as the Andean elbow region is surpassed. During its propagation into northwest Bolivia and southeast Peru, an elongated region of higher pressure builds over the eastern slopes of the Andes, aligned with the mountain range. This pressure rise seems to be a product of the incursion of denser air relative to the moist and light Amazon basin air. The establishment of the along-Andes region of high pressure provides the surge the characteristics of a barrier jet.

The characteristics of this jet can be visualized in Figure 5, through a cross section sketched at 00 UTC on January 25 2003. The cross section intercepts the Andes at 15°S and clearly illustrates the presence of the 15 m s^{-1} barrier jet and the across-mountain low-level pressure gradient with the highest pressure over the eastern slopes of the Andes (top panel). It also shows lower moisture in the region of the jet. Regardless the clear barrier jet structure, the region of the windshift is located further east in a region of moist

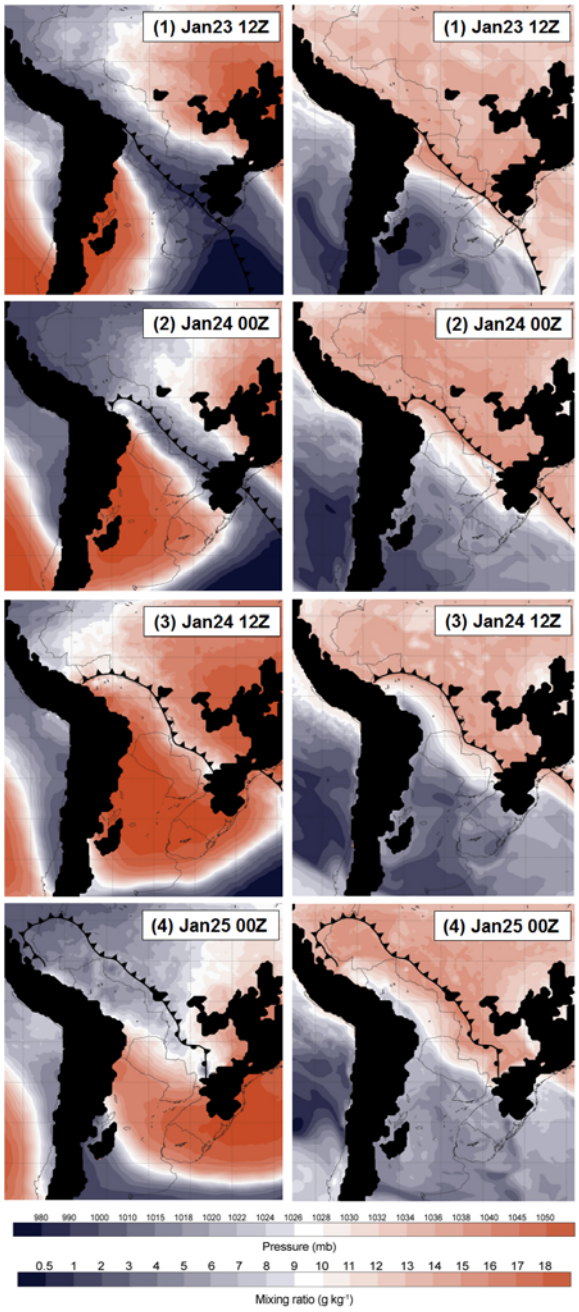

Figure 4. 925mb geopotential height in mASL (left) and mixing ratio in g kg^{-1} (right) plotted at 12 hour intervals starting temperature at 12 UTC 23 January 2003 (top panels) and ending at 00 UTC 25 January 2003 (bottom panels).

air. This suggests the presence of other mechanisms involved on the surge propagation. Among these, some kind of wave mechanism appears to be present due to the decoupling between the wind shift and the edge of the dry air observed during different stages of the surge. This decoupling is the most evident at 00 UTC 25 January (Figure 4, lowest panel), when the dry air

reaches southern Peru but the wind shift has traveled as fat north as 4°S.

The possible role of density-current propagation mechanism on the expansion of the surge away from the Andes (Figure 5) was also explored. The density current speed equation used was:

$$c^2 = 2gH\,(T_{vw}\text{-}T_{vc}/T_{vc})$$

where g is the gravity = 9.8 m s^{-1}, H the depth of the surge ~ 3000 m, T_{vw} the virtual temperature ahead of the surge and T_{vc} the virtual temperature behind the surge. The calculations indicated that speed of the surge associated a density current was in the order of 2.3 to 3.3 ° day^{-1}. This calculation is consistent with the slow northeasward expansion of the surge away from the Andes. On the other hand, the fast 9° day^{-1} meridional propagation of the surge observed between 12 UTC 24 January and 00 UTC 25 January was 3-4 times larger than the density current speeds which suggests that other mechanisms may be involved on this fast propagation.

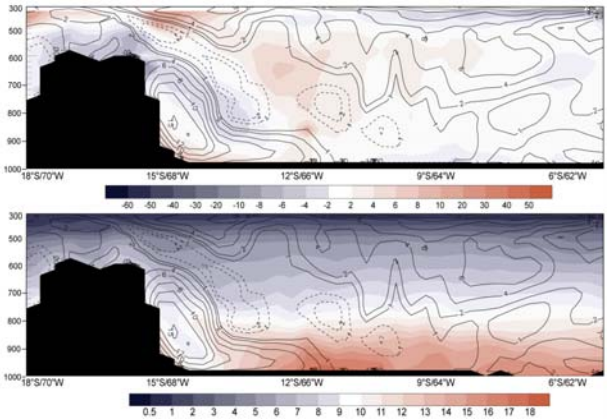

Figure 5. Vertical across-surge cross-section (#2) showing the along-surge component of the wind in m s^{-1} (contour), the geopotential height anomaly with respect to the vertical profile averaged over the cross-section in mASL (top panel, shaded) and mixing ratio in g kg^{-1} (lower panel, shaded), during January 25 2003 at 00 UTC. The edge of the wind shift is indicated. The terrain is shaded in black. The vertical coordinate is in mb.

Summary and conclusions

The southerly surge studied here was characterized by sharp changes in the wind direction along the leading edge and by the northward propagation of drier air. It seemed to encompass the characteristics of a topographically trapped downgradient flow, a barrier jet, a gravity wave and possibly a density current. During its early stages, the event behaved mainly as a topographically trapped downgradient flow driven by the strong synoptic forcing and the blocking effects of the Andes. These produced an ageostrophic component of the wind (i.e southerly flow not perpendicular to the SW-NE pressure gradient) aligned with the topographic barrier and flowing from a region of higher pressure to one of lower pressure. Effects of waves were also evident during these stages since the location of the windfield was always decoupled with the edge of the dry air. A barrier jet developed just east of the Andes and north of the Andean elbow restoring geostrophic balance by the generation of an across-barrier low-level pressure gradient. Finally, the simulated surge showed movement consistent with density current speeds along the across-surge direction, which opens the possibility that the drier air behaved as a density current in the slow northeastward expansion of the surge at low levels over the western Amazon basin.

References

Bluestein, H. B., 1993: Synoptic-Dynamic Meteorology in Midlatitudes. Oxford University Press. New York, 594 pp.

Colle, B. A., and C. F. Mass, 1995: The Structure and Evolution of Cold Surges East of the Rocky Mountains. *Mon. Wea. Rev*. **123**, 2577-2610.

Garreaud, R. D., 2000: Cold Air Incursions over Subtropical and tropical South America: Mean Structure and Dynamics. *Mon. Wea. Rev*. **128**, 2544-2559.

Garreaud, R. D., 1999: Cold Air Incursions over Subtropical and tropical South America: A Numerical Case Study. *Mon. Wea. Rev*. **127**, 2823-2853.

Garreaud, R. D. and J. M. Wallace, 1998: Summertime Incursions of Midlatitude Air into Subtropical and Tropical South America. *Mon. Wea. Rev*., **126**, 2713-2733.

Krishnamurti, T. N., M. Tewari, D. R. Chakraborty, J. Marengo, P. L. Silva Dias and P. Satyamurty. 1999: Downstream Amplification: A Possible Precursor to Major Freeze Events over Southeastern Brazil. *Weather and Forecasting*, **14**, No. 2, pp. 242–270.

Marengo, J., A. Cornejo, P. Satyamurty, and C. Nobre, 1997: Cold Surges in Tropical and Extratropical South America: The Strong Event in June 1994, *Mon. Wea. Rev*, **125**, pp 2759-2786.

Parmenter, F. C., 1976. A southern hemisphere cold frost passage at the Equador. Bulletin American Meteorological Society. 57(12): 1435-1440.

Vera, C. S., and P. K. Vigliarolo, 2000: A Diagnostic Study of Cold-Air Outbreaks over South America. *Mon. Wea. Rev*., **128**, 3-24.